EXPERIMENTAL STUDY OF NON-MEASURED POINTS ON SURFACE MEASUREMENT USING STRUCTURED ILLUMINATION MICROSCOPY

Zhen Li, Sophie Gröger

Chemnitz University of Technology, Department of Production Measuring Technology, Reichenhainer Straße 70, 09126 Chemnitz, Germany (✉ zhen.li@mb.tu-chemnitz.de, +49 371 531 375 54, sophie.groeger@mb.tu-chemnitz.de)

Abstract

Non-measured points (NMPs) are one of vital problems in optical measurement. The number and location of NMPs affect the obtained surface texture parameters. Therefore, systematic studying of the NMP is meaningful in understanding the instrument performance and optimizing measurement strategies. This paper investigates the influence of measurement settings on the non-measured points ratio (NMPR) using structured illumination microscopy. It is found that using a low magnification lens, high exposure time, high dynamic range (HDR) lighting levels, and low vertical scanning interval may help reduce the NMPR. In addition, an improved approach is proposed to analyze the influence of NMP on areal surface texture parameters. The analysis indicates that the influence of NMP on some parameters cannot be ignored, especially for extreme height parameters and feature parameters.

Keywords: non-measured points, structured illumination microscopy, areal surface texture parameters, measurement uncertainty.

1. Introduction

Surface texture parameters play an important role in controlling the surface quality of the workpiece. Surface functional performance such as wear resistance, sealing, friction, adhesion, and matching, are influenced by surface texture parameters [1]. Profile parameters [2] have been widely used for a long time. However, there is still the limitation of profile parameters because of not delivering information on the whole surface. Compared to the profile parameters, areal parameters [3] can provide a complete picture of surface information of the workpiece. However, the recent survey has shown that areal parameters are mainly used in "research institutions" and "metrology and calibration" sectors [4]. One possible reason is the lack of guidance in practical measurement

In contrast to contact methods, optical methods are more efficient in obtaining areal surface texture parameters. However, in practical measurement, various factors influence determination

of areal parameters and uncertainties for optical measurement. For example, the possible factors may be metrology characteristics of the measuring instrument [5], vibration [6], temperature fluctuations [7,8], the application of filtering [9,10], noise [11], *non-measured points* (NMPs) [12] and outliers [13].

Previous studies show that the NMP is an important problem in optical measurements. However, the study of NMP in practical measurement is limited. The NMP may be caused by too steep slopes, too high or too low light intensity due to the surface materials [6], contaminants [14], and ambient lighting [15]. *Non-measured points ratio* (NMPR) is often used to characterize the NMP. NMPR can be calculated by the number of NMPs divided by the number of total pixels. The studies also show that the measurement settings influence the NMPR [16–18]. Therefore, similarly to the measurement noise affected by the measurement settings [19], the NMPR may vary at different measurement settings.

There are many attempts to reduce the number of NMPs and their influence on surface parameters. The direct approach is to optimize the lighting source. For example, the ring light is a good option [20]. Besides, data fusion has also been used [21]. Filling the NMP with interpolation is another commonly used approach [14, 17, 22]. In addition, many measurement programs have the function of filling the NMP. However, the error is difficult to avoid. Although there are no standards to verify the filling effect, the Power Spectral Density Analysis is an approach to evaluate the filling algorithm [23].

The NMP in surface measurement has attracted much attention. However, there are still problems that need to study further. The first is that other factors may affect the NMP besides the light source, e.g., measurement settings. A systematic study of possible influences on NMP is lacking, especially for new optical measurement methods, such as *structured illumination microscopy* (SIM). The second is that how the NMP influences surface parameters is unclear. Another is that the effect of filling NMP is often ignored in practical measurement. There is no standard method to verify the filling algorithm.

Therefore, this paper studies the NMP in practical measurement using structured illumination microscopy. The aims of the study are: (1) to investigate the NMPR for different lenses, vertical scanning intervals, and exposure times, (2) to study the influence of NMP on areal surface texture parameters using an improved approach, and (3) to discuss the measurement uncertainty due to NMP.

2. Material and methods

2.1. Instrumentation and Samples

In this study, three grinding surfaces with different roughness were measured with a commercial SIM (Confovis DUO Vario Violett, Germany). The instrument principle is shown in [24]. Figure 1 is a schematic diagram of the structured illumination method used. LED A and LED B are actuated alternately during the measurement. Therefore, the image sensor captures two 180° phase-shifted images at each layer during the measurement. If the measured topography is focused, contrast difference (C) between individual images is high. However, the contrast difference (C) is low if the measured topography is not focused. Consequently, the height of the surface is determined by the contrast difference (C).

The corresponding instrument parameters are shown in Table 1. If a higher magnification objective lens is selected, the *numerical aperture* (NA) is larger. Consequently, the acceptance angle determined by the NA is also larger. However, the *field of view* (FoV) will be smaller. Apart
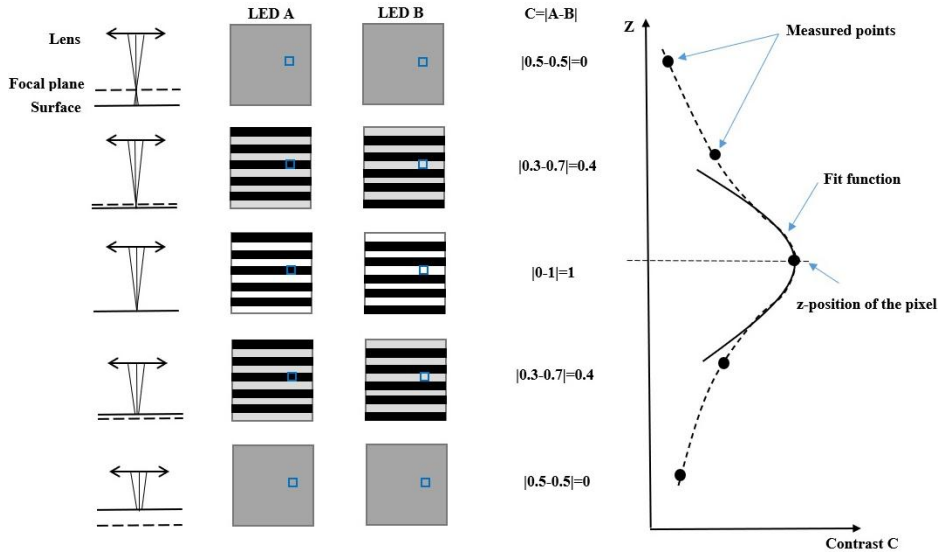
Fig. 1. Schematic diagram of the structured illumination method used [24].

from the shown parameters, the measurement software can change the light type, exposure time, and vertical scanning interval.

Table 1. Instrument parameters of the measurement system.

Lens	NA / −	Acceptance angle / °	FoV/ (µm ×µm)	Lateral sampling interval/ µm
20× magnification	0.60	36.9	630 × 630	0.248
50× magnification	0.95	71.8	254 × 254	0.099

In order to obtain surface information, there were five repeated measurements on each sample. A 20× magnification lens, 0.05 µm vertical scanning interval, and the highest exposure time without over-saturated points were used for repeated measurements. According to ISO 25178-2 standard [3], four parameters were selected to characterize the surfaces. S_q (root mean square height of the scale-limited surface) and S_z (maximum height of the scale-limited surface) indicated the surface roughness. S_{dq} (root mean square gradient of the scale-limited surface) indicated the surface complexity. S_{al} (autocorrelation length) was used to show the sharp changes in surface height.

Table 2 shows the mean values of S_q, S_z, S_{dq}, and S_{al} from five repeated measurements. The pre-process to calculate the parameters included filling the NMP by calculating a smooth shape from the neighbors, levelling the surface by subtracting the least-squares plane, and applying an

Table 2. Samples and mean values of areal surface texture parameters.

Samples	Symbols	S_q /µm	S_z /µm	S_{dq} /−	S_{al} / µm
Grinding surface 1	S_1	0.22	2.81	0.19	13.77
Grinding surface 2	S_2	0.51	5.23	0.34	8.15
Grinding surface 3	S_3	1.14	7.89	0.39	34.10

S-filter (Gaussian low-pass filter) with a nesting index of 0.8 µm. The sample's appearance and Pseudo-color view are shown in Fig. 2.
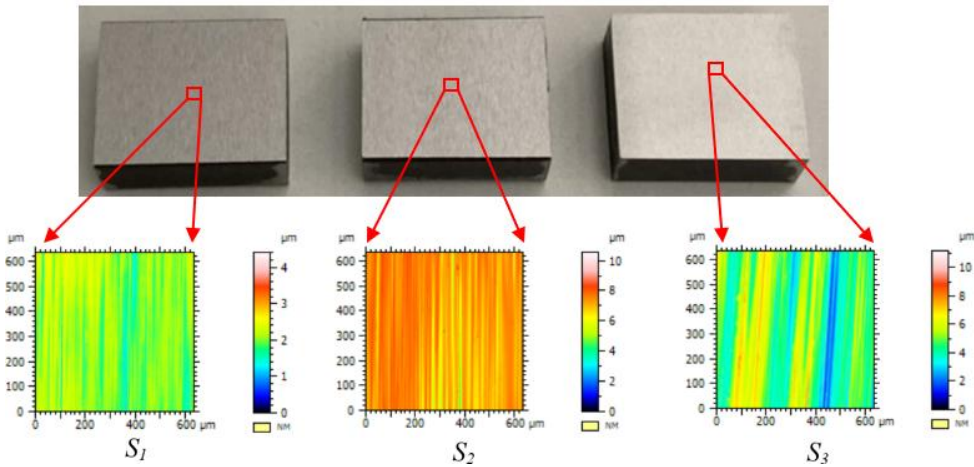

Fig. 2. The sample's appearance and Pseudo-color view.

2.2. Influence of measurement settings on NMPR

Since there was possible dispersion of the NMPR at the same measurement setting, five repeated measurements at each measurement setting were carried out. Then the mean value of NMPR was obtained to make the comparisons. In addition, a manual Goniometer Stage shown in Fig. 3 was used to eliminate the sample tilt. The sample was not moved during the measurements to guarantee that the same area was measured and compared at different measurement settings.
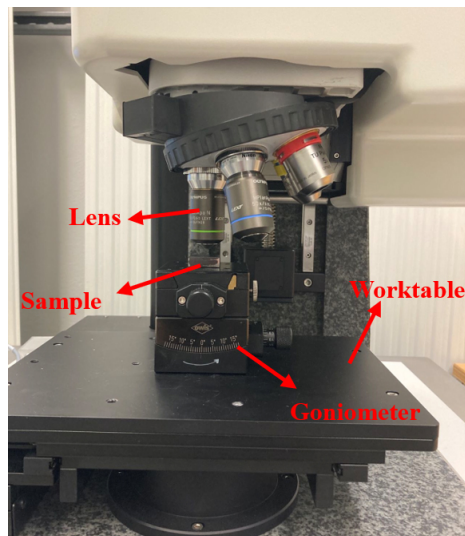

Fig. 3. The appearance of the measurement setup.

Table 3 shows the selected measurement settings. To study the NMPR at different lenses, the measurements using the highest exposure time without over-saturated points were carried out. Moreover, 0.05 μm, 0.1 μm, and 0.2 μm vertical scanning interval was selected to perform the measurements, respectively, to investigate its influence on NMPR. The highest exposure time was fixed among the vertical scanning intervals for each surface measurement. Because the FoV is different for a 20× magnification lens and a 50× magnification lens, a center 250 μm×250μm area was extracted to compare the NMPR for different lenses.

Table 3. Selected measurement settings over the measurements.

Experiment category	Sample	Lens	Exposure time / ms	Vertical scanning interval / μm
Influence of lens and vertical scanning interval	S_1	20×	1.37	0.05, 0.1, 0.2
		50×	4.54	0.05, 0.1, 0.2
	S_2	20×	1.3	0.05, 0.1, 0.2
		50×	4.58	0.05, 0.1, 0.2
	S_3	20×	1.22	0.05, 0.1, 0.2
		50×	4.32	0.05, 0.1, 0.2
Influence of exposure time	S_1	50×	2.98, 3.31, 3.68, 4.09, 4.54	0.1
	S_2	50×	3.01, 3.34, 3.71, 4.12, 4.58	0.1
	S_3	50×	2.84, 3.15, 3.50, 3.89, 4.32	0.1

To study the effect of changing exposure time on NMPR, the measurements at 0.1 μm vertical scanning interval with different exposure times were carried out. Since the exposure time can be changed in a large range when using a 50× magnification lens, the investigation was only performed with the 50× magnification lens. Measuring sample S_3 as an example, the highest exposure time without over-saturated points was 4.32 ms. Therefore, the measurements were carried out at 4.32 ms, 3.89 ms, 3.5 ms, 3.15 ms, and 2.84 ms exposure time. Moreover, *high dynamic range* (HDR) lighting levels at different vertical scanning intervals were also used to perform the measurement, which is not shown in Table 3.

2.3. Deviation estimation on areal surface texture parameters due to NMP

A commonly used approach to estimate the parameter deviation due to NMP is comparing the parameter calculated from the NMP-filled surface with the parameter calculated from the surface with NMPs. However, there may be a significant error caused by the filling precision, especially for the high NMPR surface and extreme height parameters. Therefore, based on NMP identification [23], an improved approach is proposed as follows. Figure 4 shows the process of estimating the deviation of the parameter.

Step 1. A measured surface with low NMPR was selected among different measurements. The NMP of this surface was filled, and the surface was set as a reference surface and marked as S_0. Next, the areal surface texture parameter P_0, according to ISO 25178-2, was calculated from surface S_0.

Step 2. The number and the location of other measured surfaces ($S_1, \ldots S_i$) were identified. The "NaN" represents the NMP.
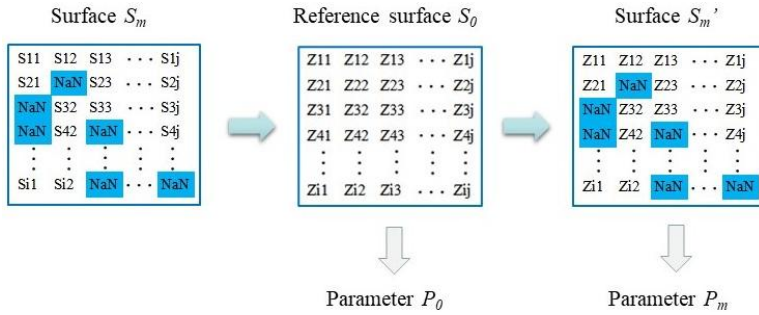
Fig. 4. The illustration of estimating parameter deviation due to NMP.

Step 3. According to the number and location of the NMPs on the surface S_i, NMPs were generated on the reference surface to get a new surface marked as S_i'. Therefore, the number and location of the NMP on the new-generated surface S_i' were the same as those on the original surface S_i. Then areal surface texture parameter P_i was calculated from surface S_i'.

Step 4. The procedure described in Step 3 several additional times was performed. The ith relative deviation (RD_i) was calculated by (1).

$$RD_i = ((P_i - P_0)/|P_0|) \times 100. \tag{1}$$

In order to verify the effectiveness of NMP filling, NMPs could be filled to get the parameter. For example, the NMPs on surface S_i' are filled to calculate parameter P_i'. The difference between the P_i' and P_0 is a measure to indicate the effectiveness of NMP filling. Moreover, based on the deviation analysis, the measurement uncertainty due to NMP can be estimated by (2).

$$U = \sqrt{\frac{1}{m} \sum_{1}^{m} (P_i - P_0)^2}, \tag{2}$$

where P_0 is the parameter calculated from the reference surface S_0, P_i is the parameter calculated from surface S_i' based on Step 3, and m is the count of repeated measurements.

3. Results and discussion

3.1. The NMPR at different measurement settings

3.1.1. NMPR at different magnification lenses

Figure 5 shows the NMPR at different magnification lenses. Except for the measurement of surface S_3 at a 0.05 µm vertical scanning interval, the NMPR was higher for the 50× lens than for the 20× lens over the measurement. The possible reason was the lateral sampling interval. The lateral sampling interval is smaller if a higher magnification lens is used. Therefore, using the 50× lens allowed to capture more fine topography details lost with a 20× lens. However, as more topography details are captured, more NMPs also exist. It is worth noting here that it does not mean the measurement quality was lower with the 50× lens.
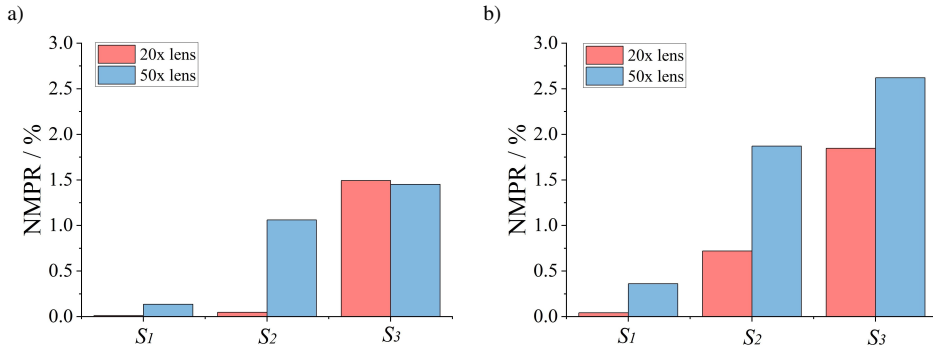
a)

b)

Fig. 5. Mean NMPR for different lenses. a) 0.05 μm vertical scanning interval and b) 0.1 μm vertical scanning interval.

3.1.2. NMPR at different vertical scanning intervals

As shown in Fig. 5, the higher the vertical scan interval, the higher the NMPR. This trend can be found clearly in Fig. 6. There was a positive correlation between the vertical scanning interval and NMPR. According to the principle of SIM shown in Fig. 1, the Z position at a pixel is calculated based on the contrast curve fit from different measured points. The scanning process captured fewer images if the vertical scanning interval was high. As a result, lower point density decreased the calculation accuracy of the height value based on a contrast curve fit. When the number of captured images was too small, there was insufficient information to fit the contrast curve to determine the Z position at specific pixels. These points were flagged as NMPs by the measurement system. Usually, the instrument manual suggests the required minimum of captured images during the scanning.
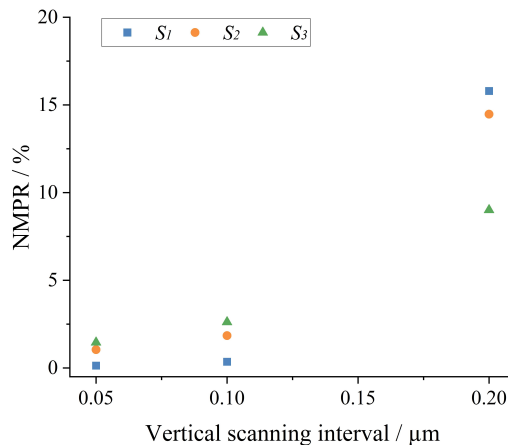

Fig. 6. Mean NMPR at different vertical scanning intervals for the 50× lens.

3.1.3. NMPR at different exposure times

The NMPR at different exposure times is shown in Fig. 7. The NMPR decreased significantly with the increase of the exposure time. There are deep valleys and scratches on rough surfaces. Increasing exposure time allows to detect more information about these areas. For example, Fig. 8

shows an extracted valley area of surface S_3 measured for the 50× lens. The number of NMPs was 32528 when the exposure time was 2.84 ms. However, the number of NMPs decreased to 4758 when the exposure time was 4.32 ms.
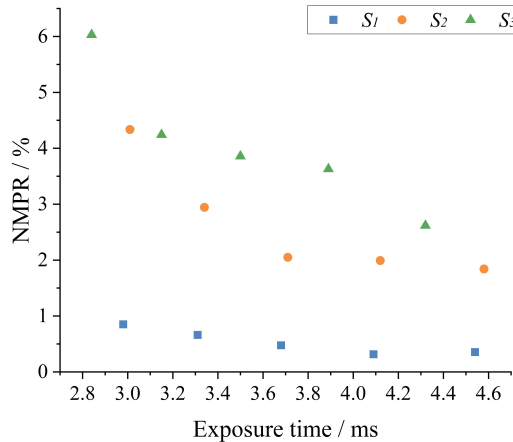

Fig. 7. Mean NMPR at different exposure times for the 50× lens.
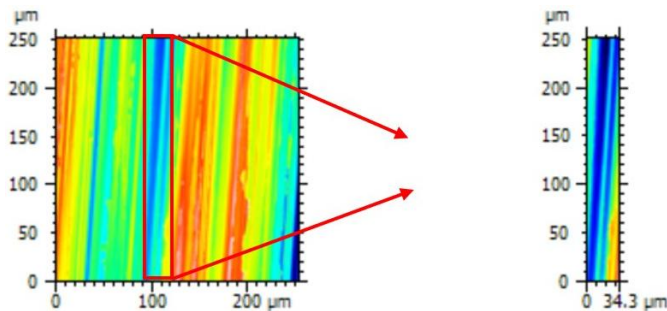

Fig. 8. An extracted valley area of surface S_3.

Although increasing exposure time can to some extent decrease NMPR, it may cause over-saturated points at some peaks or high reflective areas. Therefore, there is an ideal exposure time to obtain the lowest NMPR in the practical measurement. The exposure time can be adjusted based on the materials and structure features to decrease NMPR. It should be noted that if the high slope on the surface causes NMPs, the effectiveness of increasing exposure time is limited due to the acceptance angle of the lens.

Figure 9 shows that the NMPR decreased if HDR lighting levels were used. HDR lighting levels mean the measurement is carried out at different exposure times. Then the measurement results are merged. It is an option to improve the measurement when the surface contains different reflective areas. These areas could not be well detected if a single exposure time was used. However, the HDR lighting levels could make more areas well detected and reduce the NMPR. For example, the NMPR of surface S_2 measurement was 1.84% at a 0.1 μm vertical scanning interval and with the highest possible exposure time set. The NMPR decreased to 0.7% when

the HDR lighting levels were used. It shows that the NMPR was significantly reduced due to the HDR lighting levels.
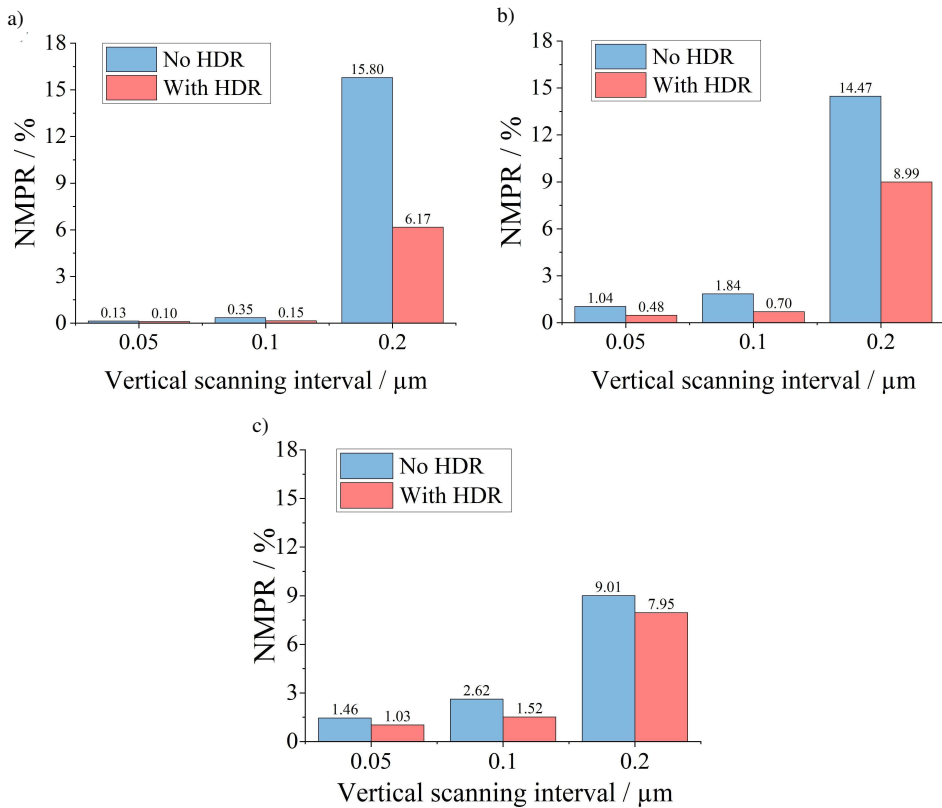

Fig. 9. Mean NMPR at HDR lighting levels. a) Surface S_1, b) Surface S_2, and c) Surface S_3.

It should be noted that, as seen in Fig. 9, the HDR lighting levels may only decrease the NMPR to a limited extent in some cases. The reason is that the HDR lighting levels can not significantly reduce the NMP caused by the high slopes. Furthermore, using HDR lighting levels required more measurement time because of the multiple measurements. Therefore, using the HDR lighting levels to decrease the NMPR should be balanced in the practical measurement.

3.2. Influence of NMP on areal surface texture parameters

As discussed above, NMPR varies for different measurement settings. In order to simplify the investigation of NMP on areal surface texture parameters, only five different NMPRs for the 50× lens were selected for each sample, as shown in Table 4. These NMPRs vary in exposure time and vertical scanning interval. Because of the lowest NMPR, a surface measured at 0.05 µm vertical scanning interval was filled and then set as the reference surface for each sample. In this section, the areal surface texture parameters were calculated by the MountainsMap software.

Figure 10 shows the highest deviation of areal surface texture parameters due to NMPs. If the relative deviation of one parameter was the highest at a surface, the NMPs on this surface

Table 4. Selected NMPRs for the 50× lens.

Samples	NMPR / %
S_1	0.13, 1.17, 8.49, 18.68, 26.84
S_2	1.03, 2.95, 5.29, 13.05, 18.28
S_3	1.45, 3.53, 5.56, 8.59, 9.7

were also filled to calculate the parameter to verify the effect of the filling. Taking surface S_1 as an example, the highest deviation of S_q was –2.15%, which was at the surface with NMPR equal to 26.84%. Then NMPs on this surface were filled, and S_q was calculated again; the relative deviation of S_q changed to –0.46%.

The results show that the influence of NMPs on S_q and S_a was insignificant, even though the NMPR might be high. It is logically valid because the S_q and S_a represent height variation for the entire surface. They are statistical parameters. Usually, the NMPs are distributed on the whole surface and are not located in only one area. Therefore, the NMP affects some height values but cannot significantly affect the whole surface's height variation. For sample S_1 and sample S_2, the highest deviation of S_q and S_a was on the surface with the highest NMPR. However, for sample S_3, the highest deviation of S_q and S_a was not on the surface with the highest NMPR. It indicates that the influence of NMP on the areal surface texture parameters depends on the number and location.

S_{sk} and S_{ku} are measures of surface height distribution. The highest deviation due to NMPs was on the surface, with the highest NMPR for each sample. The reason is that if there are a large number of NMPs at the valleys and peaks, the surface height distribution will be significantly affected. The highest NMPR of sample S_3 was smaller than samples S_1 and S_2. Therefore, the relative deviation of S_{ku} for sample S_3 was smaller. However, the relative deviation of S_{sk} for sample S_3 was huge. The reason was that the S_{sk} of sample S_3 was only -0.018, and a slight absolute deviation could also cause a sizeable relative deviation.

S_p is the largest peak height value, S_v is the largest pit height value, and S_z is the sum of S_p and S_v. If there are NMPs located at peaks, S_p will generally decrease. If there are NMPs located in valleys, S_v will generally decrease. It should be noted that S_p and S_v may increase slightly due to NMPs. The possible reason is the influence of noise filtering. Because two single points among the whole surface determined the parameters, the location of the NMP has much impact on the parameters.

S_{al} is a measure of sharp changes in surface height, and S_{tr} is a measure of the presence of lay. As seen in Fig. 10, the relative deviation of S_{al} and S_{tr} was low. The reason was no sharp surface height change and no significant lay distribution change due to NMPs in the selected cases. However, if the surface was slashed significantly due to NMP concentration in a particular area, the S_{al} and S_{tr} would be substantially affected.

S_{mc} and S_{xp} belong to functional parameters. For S_{mc}, the largest deviation appeared at the surface with the highest NMPR for each sample. However, for S_{xp}, the largest deviation only appeared at the surface with the highest NMPR for sample S_1. This is because S_{mc} and S_{xp} depend on the shape of the Abbott–Firestone curve. Figure 11 shows the Abbott–Firestone curve of a surface S_1 for different NMP conditions. The upper left of the curve indicates the field with reduced peak heights, and the lower right of the curve indicates the field with reduced valley depths. In other words, the peak heights affect the upper left curve, and the valley depths affect the lower right curve. Suppose the NMPs are located in different areas. In that case, the curve shape changes significantly. As shown in Fig. 11, the lower right curve changes due to the NMPs
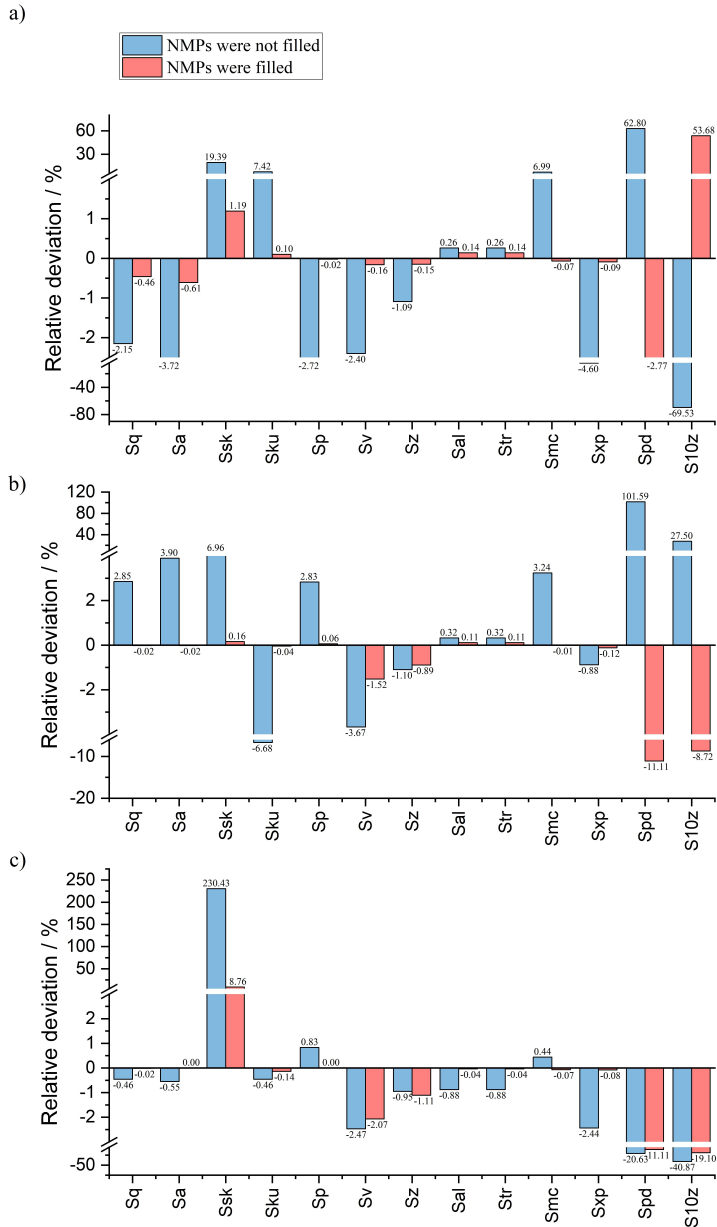
Fig. 10. The highest relative deviation of areal texture parameters due to NMPs. (a) S_1, (b) S_2, and (c) S_3.

at valleys, and the upper left of the curve changes due to the NMPs at peaks. Therefore, there was a deviation of S_{mc} and S_{xp}. It should be noted that other functional parameters also depend on the Abbott–Firestone curve.

S_{pd} and S_{10z} are feature parameters. According to the definition, feature parameters reflect the features of the surface. This is different from the height parameters that reflect the points on
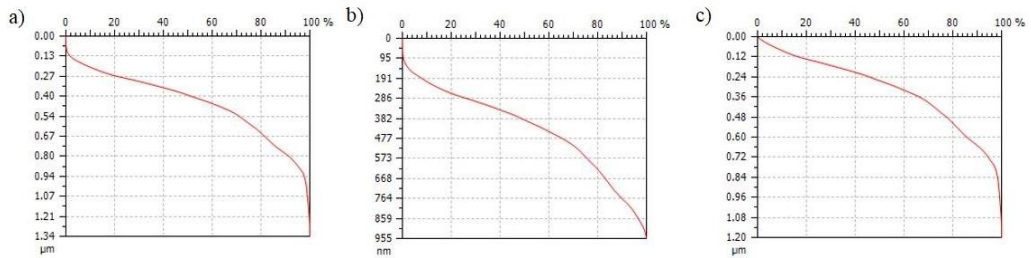
Fig. 11. Abbott–Firestone curve of S_1. a) 0% NMP, b) 2% NMPR located in valleys, and c) 2% NMPR located at peaks.

the surface. The existence of NMPs may significantly change the distribution of features such as peaks, saddles, and pits. Taking Motifs analysis of sample S_3 as an example, if there were no NMPs on the surface, 69 peaks and 78 pits were detected, respectively. However, when the NMPR was 5.56%, 403 peaks and 413 pits were detected because the NMPs separated the surface into more areas. The results show that the number of peaks and pits changed significantly due to the NMPs. Accordingly, the statistic height of the peaks and pits also considerably changed. That was the possible reason why S_{pd} and S_{10z} varied significantly due to NMPs.

Figure 10 also shows that filling the NMPs helped obtain relative accurate areal surface texture parameters. For example, the deviation of S_a of sample S_3 even decreased to zero after filling the NMPs. However, in some cases, such as feature parameters, the deviation was still high after filling the NMPs. Therefore, filling precision should be investigated if the NMPs are filled before parameter calculation. It is worth noting that in some cases the highest NMPR does not mean the largest deviation of parameters. Therefore, judging the parameter deviation directly from NMPR is not recommended.

3.3. Uncertainty estimation

In this section, the height parameters of S_1 and S_3 are considered as an example to show the uncertainty estimation. Ten repeated measurements with the 20× lens, at the 0.1 μm vertical scanning interval and the highest available exposure time were carried out. The measurement uncertainty due to NMP during the repeated measurements is shown in Table 5.

The uncertainty in Table 5 was calculated according to Section 2.3. Among the ten repeated measurements, the surface with the lowest NMPR was selected as the reference surface. Then NMPs on this reference surface were filled. Consequently, the parameters were calculated. These parameters were considered reference values. Next, the position and number of NMPs were identified for each measured surface. Based on the known NMP information, the NMPs were generated on the reference surface. Therefore, ten new surfaces were created. Next, the parameters of these ten new-generated surfaces were calculated and compared to the parameters calculated from the reference surface. Finally, the uncertainty was obtained by (2).

The third column of Table 5 was the uncertainty when the NMPs on the new-generated surfaces were not filled. The fourth column shows the uncertainty when the NMPs on the new-generated surfaces were filled.

The results show that the uncertainty of S_q, S_a, S_{sk}, and S_{ku} was low regardless of the samples. The reason was that the NMPR was relatively low, and the surface height distribution was not significantly affected by NMPs. However, the uncertainty of S_p, S_v, and S_z was high and could be up to hundreds of nanometers. The reason was S_p, S_v, and S_z were determined by two

Table 5. Measurement uncertainty due to NMPs during the repeated measurements.

Samples	Parameters	NMPs were not filled	NMPs were filled
S_1	S_q/ nm	0.04	0.01
	S_{sk}/ −	0.001	0.001
	S_{ku}/ −	0.002	0.002
	S_p/ nm	0.09	0.01
	S_v/ nm	310.74	206.99
	S_z/ nm	310.80	206.98
	S_a/ nm	0.03	0.01
S_3	S_q/ nm	5.68	0.22
	S_{sk}/ −	0.004	0.001
	S_{ku}/ −	0.005	0.001
	S_p/ nm	356.19	224.79
	S_v/ nm	192.50	157.60
	S_z/ nm	540.22	374.43
	Sa/ nm	4.87	0.22

single points. Therefore, the NMPs can have a significant impact on these parameters. It should be noted that the location of NMPs has more influence on the measurement uncertainty of S_p, S_v, and S_z.

It is found that filling NMPs helps to decrease the measurement uncertainty of height parameters, especially for S_q, S_a, S_{sk}, and S_{ku}. However, the uncertainty of S_p, S_v, and S_z was still up to hundreds of nanometers. Therefore, because of the NMPs, accurate measurement of S_p, S_v, and S_z is challenging for optical measurement. Thus, the influence of NMPs should be considered for the uncertainty estimation.

This section only considers the influence of NMPs on height parameters among the repeated measurements. However, this approach can also obtain uncertainty due to NMPs at other areal surface texture parameters. It should be noted that the filling algorithm also influences the uncertainty evaluation if the NMPs are filled before parameter calculation.

4. Conclusions

In this paper, three grinding surfaces were measured at different measurement settings using SIM. The measurement settings include different magnification lenses, exposure times, and vertical scanning intervals. A systematic investigation of the influence of measurement settings on NMPR was made. Moreover, an improved approach to analyzing the influence of NMP on areal surface texture parameters was proposed. Finally, the uncertainty evaluation of height parameters due to NMPs was shown.

The investigation shows that the lens, exposure times, and vertical scanning interval significantly influence the NMP. Overall, using a low magnification lens, high exposure time, low vertical scanning interval, and HDR lighting levels helps to reduce the NMPR in the studied cases.

The influence of NMPs on areal surface texture parameters depends not only on the number of NMPs but also on their location. The influence of NMPs on statistical parameters such as S_q and S_a is insignificant. However, the influence of NMPs on extreme height parameters and feature parameters is significant. For example, S_p, S_v, S_z, S_{pd} and S_{10z} may significantly deviate due to NMPs. Filling NMPs is an option to reduce the parameter deviation. However, the effect of the filling may be limited for the above-mentioned extreme height and feature parameters.

Accordingly, the study shows that the measurement uncertainty of S_a, S_q, S_{sk}, and S_{ku} due to NMPs is low for the height parameters. However, the measurement uncertainty of S_p, S_v, and S_z is high. The proposed approach is feasible to estimate the uncertainty of other areal surface parameters.

References

[1] Leach, R. (Ed.). (2013). *Characterisation of Areal Surface Texture*. Springer Science & Business Media.

[2] International Organization for Standardization. (1997). *Geometrical Product Specifications (GPS) – Surface texture: Profile method – Terms, definitions and surface texture parameters* (ISO 4287:1997). https://www.iso.org/standard/10132.html

[3] International Organization for Standardization. (2012). *Geometrical product specifications (GPS) – Surface texture: Areal – Part 2: Terms, definitions and surface texture parameters* (ISO 25178-2:2012). https://www.iso.org/standard/42785.html

[4] Todhunter, L. D., Leach, R. K., Lawes, S. D., & Blateyron, F. (2017). Industrial survey of ISO surface texture parameters. *CIRP Journal of Manufacturing Science and Technology, 19*, 84–92. https://doi.org/10.1016/j.cirpj.2017.06.001

[5] International Organization for Standardization. (2020). *Geometrical product specifications (GPS) – Surface texture: Areal – Part 700: Calibration, adjustment and verification of areal topography measuring instruments* (ISO/DIS 25178-700:2020).

[6] Leach, R. (Ed.). (2011). *Optical Measurement of Surface Topography* (Vol. 8). Springer Berlin Heidelberg.

[7] Miller, T., Adamczak, S., Świderski, J., Wieczorowski, M., Łętocha, A., & Gapiński, B. (2017). Influence of temperature gradient on surface texture measurements with the use of profilometry. *Bulletin of the Polish Academy of Sciences. Technical Sciences*, *65*(1). https://doi.org/10.1515/bpasts-2017-0007

[8] Grochalski, K., Wieczorowski, M., Pawlus, P., & H'Roura, J. (2020). Thermal sources of errors in surface texture imaging. *Materials*, *13*(10), 2337. https://doi.org/10.3390/ma13102337

[9] He, B., Ding, S., Wei, C., & Shi, Z. (2021). The Influence of the Choice of a Gaussian Filter on the Determination of Areal Surface Texture Parameters. *Instruments and Experimental Techniques, 64*(1), 71–77. https://doi.org/10.1134/S0020441220060160

[10] He, B., Zheng, H., Ding, S., Yang, R., & Shi, Z. (2021). A review of digital filtering in surface roughness evaluation. *Metrology and Measurement Systems*, *28*(2). https://doi.org/10.24425/mms.2021.136606

[11] Podulka, P. (2020). Proposal of frequency-based decomposition approach for minimization of errors in surface texture parameter calculation. *Surface and Interface Analysis, 52*(12), 882–889. https://doi.org/10.1002/sia.6840

[12] Pawlus, P., Reizer, R., & Wieczorowski, M. (2017). Problem of non-measured points in surface texture measurements. *Metrology and Measurement Systems*, *24*(3), 525–536. https://doi.org/10.1515/mms-2017-0046

[13] Wang, C., D'Amato, R., & Gómez, E. (2019). Confidence Distance Matrix for outlier identification: A new method to improve the characterizations of surfaces measured by confocal microscopy. *Measurement, 137*, 484–500. https://doi.org/10.1016/j.measurement.2019.01.043

[14] Leach, R. K., Brown, L., Jiang, X., Blunt, R., Conroy, M., & Mauger, D. (2008). *Guide to the measurement of smooth surface topography using coherence scanning interferometry*. http://eprints publications.npl.co.uk/id/eprint/4099

[15] Rachakonda, P., Muralikrishnan, B., & Sawyer, D. (2019, May). Sources of errors in structured light 3D scanners. *In Dimensional Optical Metrology and Inspection for Practical Applications VIII* (Vol. 10991, p. 1099106). International Society for Optics and Photonics. https://doi.org/10.1117/12.2518126

[16] Newton, L., Senin, N., Gomez, C., Danzl, R., Helmli, F., Blunt, L., & Leach, R. (2019). Areal topography measurement of metal additive surfaces using focus variation microscopy. *Additive Manufacturing, 25*, 365–389. https://doi.org/10.1016/j.addma.2018.11.013

[17] Feng, X., Senin, N., Su, R., Ramasamy, S., & Leach, R. (2019). Optical measurement of surface topographies with transparent coatings. *Optics and Lasers in Engineering*, *121*, 261–270. https://doi.org/10.1016/j.optlaseng.2019.04.018

[18] Gomez, C., Su, R., Thompson, A., DiSciacca, J., Lawes, S., & Leach, R. K. (2017). Optimization of surface measurement for metal additive manufacturing using coherence scanning interferometry. *Optical Engineering, 56*(11), 111714. https://doi.org/10.1117/1.OE.56.11.111714

[19] Li, Z., & Gröger, S. (2021). Investigation of noise in surface topography measurement using structured illumination microscopy. *Metrology and Measurement Systems*, *28*(4). https://doi.org/10.24425/mms.2021.137706

[20] Liu, W., Chen, X., Zeng, W., Sun, W., Jiang, X., Scott, P., & Lou, S. (2021, September). FVM and XCT Measurement of Surface Texture of Additively Manufactured Parts. *In 2021 26th International Conference on Automation and Computing (ICAC)* (pp. 1–6). IEEE. https://doi.org/10.23919/ICAC50006.2021.9594146

[21] Bermudez, C., Matilla, A., & Aguerri, A. (2017). Confocal fusion: Towards the universal optical 3D metrology technology. *Proceedings of the 12th LAMDAMAP, Renishaw Innovation Center, Wotton-Under-Edge, UK*, 15-16. http://www.euspen.eu/knowledge-base/LAM138.pdf

[22] Kapłonek, W., Nadolny, K., & Królczyk, G. M. (2016). The use of focus-variation microscopy for the assessment of active surfaces of a new generation of coated abrasive tools. *Measurement Science Review*, *16*(2), 42–53. https://doi.org/10.1515/msr-2016-0007

[23] Flys, O., Berglund, J., & Rosén, B. G. (2020). Using confocal fusion for measurement of metal AM surface texture. Surface Topography. *Metrology and Properties, 8*(2), 024003. https://doi.org/10.1088/2051-672X/ab84c3

[24] Confovis GmbH. (n.d.). *Structured Illumination Microscopy*. Retrieved September 18, 2022. https://www.confovis.com/en/optical-measurement

Zhen Li received his B. Eng. degree and M. Eng. degree from Hefei University of Technology, China, in 2006 and 2013, respectively. He is currently pursuing a Ph.D. degree at Chemnitz University of Technology, Germany. His main research interest are precision measurement technology and instruments.

Sophie Gröger received her Ph.D. degree from Chemnitz University of Technology, Germany, in 2007. She is currently Full Professor and Head of the Production Measuring Technology Department at Chemnitz University of Technology. Her current research interests include Geometrical Product Specification and optical as well as tactile geometrical measurements. She is a member of national and international standardization committees on Geometrical Product Specification and Verification.